COMPARISON OF ACTIVE NOISE CONTROL STRUCTURES IN THE PRESENCE OF ACOUSTICAL FEEDBACK BY USING THE H_∞ SYNTHESIS TECHNIQUE

M. R. Bai and H. H. Lin

Department of Mechanical Engineering, Chiao-Tung University, 1001 Ta-Hsueh Rd., Hsin-Chu, Taiwan, Republic of China

This study compares three control structures of active noise cancellation for ducts: feedback control, feedforward control, and hybrid control. These structures are compared in terms of performance, stability, and robustness by using a general framework of the H_∞ robust control theory. In addition, the H_∞ synthesis procedure automatically incorporates the acoustic feedback path that is usually a plaguing problem to feedforward control design. The controllers are implemented by using a digital signal processor and tested on a finite-length duct. In an experimental verification, the proposed controllers are also compared with the well-known filtered-*u* least mean square (FULMS) controller. The advantages and disadvantages of each ANC structure as well as the adverse effects due to acoustic feedback are addressed.

© 1997 Academic Press Limited

1. INTRODUCTION

Active noise control (ANC) techniques complement traditional methods for suppressing low frequency disturbances [1, 2]. In the ANC applications up to date, feedforward control has been widely used whenever a non-acoustical reference signal has been available. In particular, the least mean square (LMS) method and its variants have formed the majority of the ANC approaches [3–5]. However, this does not preclude the use of the other structures that have been well established in the control community. This paper is aimed to compare three ANC structures (feedforward structure, feedback structure, and hybrid structure) on the basis of the H_∞ theory [6–11]. Important issues such as performance, stability, and robustness are all taken simultaneously into account in the H_∞ design. In addition, the H_∞ synthesis procedure automatically incorporates the acoustic feedback path that is usually a plaguing problem to ANC applications. Acoustic feedforward usually arises in feedforward ANC structure for suppressing broadband random noises, where in many practical situations only the acoustical noise reference is available. In this configuration, a positive feedback loop exists between the cancelling loudspeaker and the feedback microphone, which tends to destabilize an ANC system. Acoustic feedback introduces poles to the system and thus stability problems if the loop gain becomes too large. An excellent review concerning acoustic feedback can be found in the book by Kuo and Morgan [12]. The solutions to the problem of acoustic feedback mentioned in the book include directional microphones and loudspeakers, motional feedback loudspeakers, neutralization filter, dual-microphone reference sensing, filter-*u* LMS (FULMS) method, non-acoustic sensors, and so forth. In contrast, this paper adopts a new approach based

on H_∞ theory to explore the acoustic feedback problem in the ANC application domain from the standpoint of control theories.

The H_∞ controllers are implemented by using a floating-point digital signal processor (DSP) and tested on a finite-length duct. Various types of noises including a Gaussian white noise, an engine exhaust noise, an impact noise, and a sweep-sine were chosen for validating the control structures. As will be seen in the experimental results, the problem of acoustic feedback is successfully dealt with by the hybrid H_∞ controller that provides marked improvement of performance and robustness over the feedforward H_∞ controller, the feedback H_∞ controller, and the well-known filter-u least mean square algorithm (FULMS) that has long been recognized as an effective solution to the acoustic feedback problem [4]. The advantages, disadvantages, and design considerations indicated in the experimental results for each ANC structure are summarized in the conclusion.

2. THEORIES AND METHODS

2.1. H_∞ CONTROL THEORY

In this paper, the H_∞ robust control theory based on two Riccati equations (the so-called 1988 approach) is employed for controller synthesis because it provides a unified framework for all control structures [6–11]. In addition, the H_∞ theory reveals physical insights into the perturbations and uncertainties of models that result from system identification, aging of electronic components, environmental changes, non-linearity, and drifting of acoustic system properties that generally arise in practical applications. These factors might cause deterioration of performance or even stability. It is then desirable to develop an ANC controller capable of accommodating these detrimental effects. To this end, the H_∞ control theory is employed to meet the requirements of robust performance and robust stability in the face of plant uncertainties by choosing proper weighting functions.

In modern control theory, all control structures can be described by using a generalized control framework, as depicted in Figure 1. The variables and functions in the Z domain are all capitalized. The framework contains a controller $C(z)$ and an *augmented plant $P(z)$*. The controlled variable $v(k)$ corresponds to various control objectives $z_1(k)$, $z_2(k)$ and $z_3(k)$, and the extraneous input $w(k)$ consists of the reference $r(k)$, the distubance $d(k)$, and the noise $n(k)$. The signals $u(k)$ and $e(k)$ are the control input to the plant and the measured output from the plant, respectively. The general input–output relation can be expressed as

$$\begin{bmatrix} V(z) \\ E(z) \end{bmatrix} = \begin{bmatrix} P_{11}(z) & P_{12}(z) \\ P_{21}(z) & P_{22}(z) \end{bmatrix} \begin{bmatrix} W(z) \\ U(z) \end{bmatrix} = P_\gamma(z) \begin{bmatrix} W(z) \\ U(z) \end{bmatrix}, \tag{1}$$
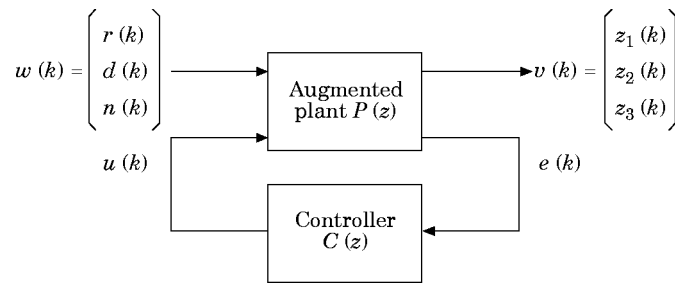

Figure 1. Generalized control framework.

where the submatrices $P_{ij}(z)$, $i, j = 1, 2$ are compatible partitions of the augmented plant $P_\gamma(z)$, and the signal variables are capitalized to represent the symbols in the Z domain.

The rationale of the H_∞ control is to minimize the infinity norm of the transfer function $T_{VW}(z)$ between $v(k)$ and $w(k)$, where the infinity norm represents the output energy (in ℓ_2 norm) for the worst input of energy less than or equal to unity. It is straightforward to show that $T_{vw}(z)$ can be expressed as [10]

$$T_{VW}(z) = P_{11}(z) + P_{12}(z)C(z)\,[1 - P_{22}(z)C(z)]^{-1}P_{21}(z). \tag{2}$$

Hence, the mathematical statement of the optimal H_∞ problem reads

$$\min_{C(z)} \| T_{VW}(z) \|_\infty = \min_{C(z)} \sup_{0 \leqslant \theta < 2\pi} \| T_{VW}(e^{j\theta}) \|. \tag{3}$$

With the optimal H_∞ controller, best tracking performance, disturbance, rejection, and uncertainty accommodation can be achieved under the condition that the whole system is internally stable. However, instead of the optimal solution that is generally very difficult to find, one is content with the suboptimal solution of the so-called *standard H_∞* problem: finding $C(z)$ such that $\| T_{VW}(z) \|_\infty < 1$.

2.2. CONTROL STRUCTURES

In this section, the feedback structure, the feedforward structure, and the hybrid structure are formulated on the basis of the aforementioned generalized control framework. In the feedforward and hybrid structure, it is further assumed that only the acoustical reference at the upstream of the canceling source is available, as usually is the case in practical applications. Because the upstream feedforward microphone will pick up both the noise from the primary source and the noise produced by the canceling loudspeaker, the positive acoustic feedback problem can no longer be ignored. It is this positive feedback problem that considerably complicates the active control design and so limits the performance and stability of the ANC system.

First, the feedback structure is illustrated in Figure 2. To find an H_∞ controller, one weighs the error signal $e(k)$ by $W_1(z)$, the control input $u(k)$ by $W_2(z)$, and the plant output $y(k)$ with $W_3(z)$. At this point, it is relevant to introduce two important sensitivity functions: the sensitivity function $\tilde{S}(z)$ and the complementary sensitivity function $\tilde{T}(z)$ defined as [9]

$$\tilde{S}(z) = 1/[1 + P_2(z)C(z)] \tag{4}$$

and

$$\tilde{T}(z) = P_2(z)C(z)/[1 + P_2(z)C(z)]. \tag{5}$$

The sensitivity functions $\tilde{S}(z)$ and $\tilde{T}(z)$ are, respectively, the indices of the system's ability to cope with disturbances and uncertainties [9]. For good disturbance rejection, the normal performance condition must be satisfied

$$\| \tilde{S}(z)W_1(z) \|_\infty < 1. \tag{6}$$

On the other hand, to maintain stability of the system against plant perturbations and model uncertainties, the robustness condition that can be derived from the *small-gain* theorem must be satisfied [9]

$$\| \tilde{T}(z)W_3(z) \|_\infty < 1. \tag{7}$$

In general, $W_1(z)$ is chosen as a lowpass function and $W_3(z)$ is chosen as a highpass function because the low frequency performance of disturbance rejection in the control
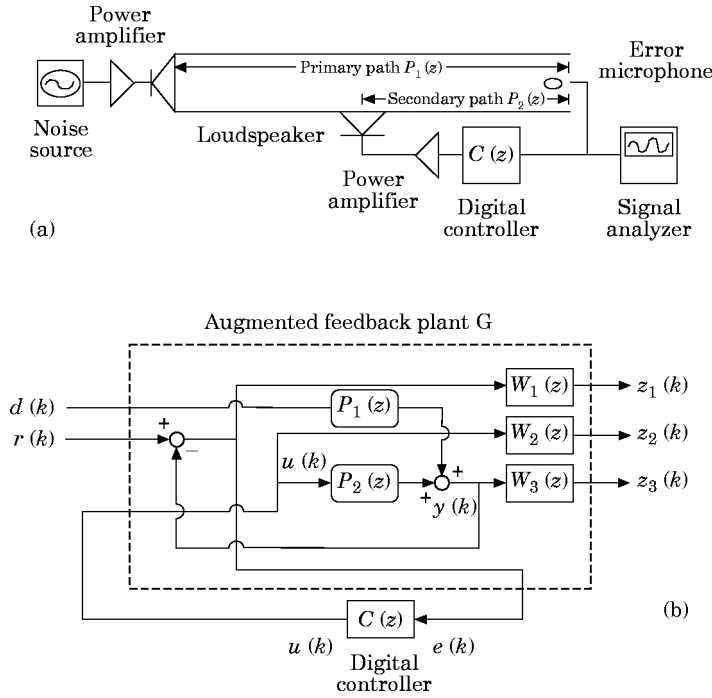
Figure 2. Feedback ANC structure: (a) experimental setup; (b) block diagram.

band is more of a concern and plant uncertainties tend to fall in high frequencies due to, for example, modal truncation. It is yet very difficult to simultaneously minimize both sensitivity functions by simply noting that $\tilde{S}(z) + \tilde{T}(z) = 1$. The tradeoff between $\tilde{S}(z)$ and $\tilde{T}(z)$ is further complicated by the *waterbed* effect. That is, one cannot minimize either sensitivity function in a frequency range without inducing amplification of the same function at the other frequencies if the plant is at non-minimum phase [10]. This classical tradeoff between the performance and robustness renders the following *mixed sensitivity* problem [9]

$$\| \, |\tilde{S}(z)W_1(z)| + |\tilde{T}(z)W_3(z)| \, \|_\infty < 1. \tag{8}$$

The input–output relation of the augmented plant corresponding to the feedback structure is

$$\begin{bmatrix} Z_1(z) \\ Z_2(z) \\ Z_3(z) \\ E(z) \end{bmatrix} = \begin{bmatrix} W_1(z) & -W_1(z)P_2(z) \\ 0 & W_2(z) \\ 0 & W_3(z)P_2(z) \\ 1 & -P_2(z) \end{bmatrix} \begin{bmatrix} D(z) \\ U(z) \end{bmatrix}, \tag{9}$$

where $P_1(z)$ is the primary path and $P_2(z)$ is the secondary path. Hence, the suboptimal condition of the feedback controller can be shown to be

$$\left\| \begin{bmatrix} W_1(z)\tilde{S}(z) \\ W_2(z)R(z) \\ W_3(z)\tilde{T}(z) \end{bmatrix} \right\|_\infty < 1, \tag{10}$$

where $\tilde{S}(z)$ and $\tilde{T}(z)$ are defined by equations (4) and (5), and $R(z) = C(z)/[1 + P_2(z)C(z)]$. The additional weighting function $W_2(z)$ is used to limit the control input $u(k)$ and is generally chosen to be a small constant.

Next, consider the acoustic feedback problem. As has been mentioned previously, acoustic feedback generally causes detrimental effects to the ANC systems whenever feedforward sensors are used, such as the feedforward structure and the hybrid structure in our case. However, it will become clear later that acoustic feedback is naturally incorporated into the H_∞ synthesis procedure. Indeed, the merit of the H_∞ general framework lies in the fact that it does not require special treatment insofar as acoustic feedback is concerned. The block diagram of the feedforward structure with acoustic feedback is illustrated in Figure 3. The input–output relation of the augmented plant corresponding to the feedforward structure is

$$\begin{bmatrix} Z_1(z) \\ Z_2(z) \\ E(z) \end{bmatrix} = \begin{bmatrix} W_1(z)P_1(z) & W_1(z)P_2(z) \\ 0 & W_2(z) \\ 1 & P_3(z) \end{bmatrix} \begin{bmatrix} D(z) \\ U(z) \end{bmatrix}, \tag{11}$$

where $P_3(z)$ is the transfer function of the acoustic feedback path. Dropping (z) for convenience, the suboptimal condition of the H_∞ feedforward controller can be shown to be

$$\left\| \begin{bmatrix} W_1 FS \\ W_2 FR \end{bmatrix} \right\|_\infty < 1, \tag{12}$$

where

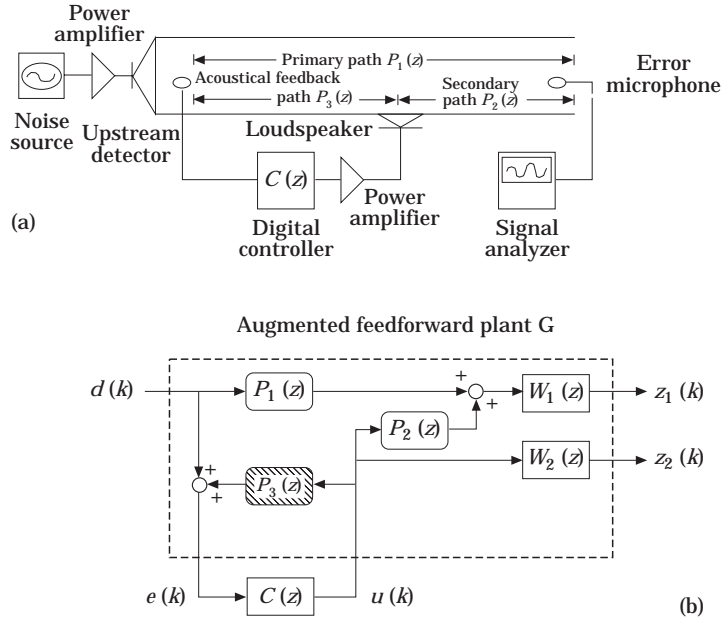$$FS = P_1(1 - CP_3) + CP_2/(1 - CP_3), \qquad FR = C/(1 - CP_3).$$

Figure 3. Feedforward ANC structure including an acoustical feedback path: (a) experimental setup; (b) block diagram. The shaded block indicates the acoustic feedback path.
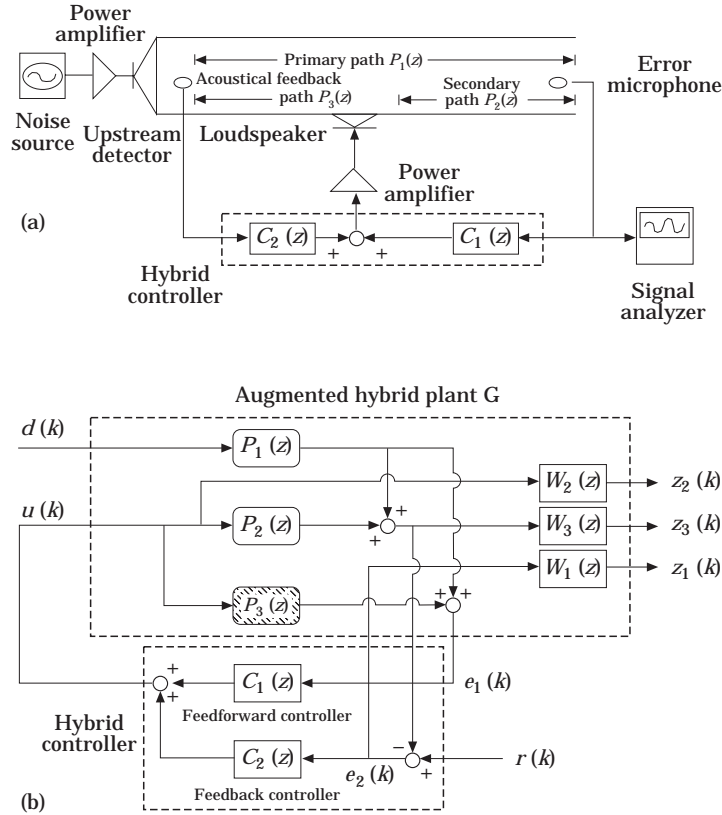
Figure 4. Hybrid ANC structure including an acoustical feedback path: (a) experimental setup; (b) control block diagram. The shaded block indicates the acoustic feedback path.

$FS(z)$ is the transfer function from the disturbance to the output. To achieve good disturbance rejection, $FS(z)$ should be small in the present low frequency control band. The downstream microphone output is weighed by $W_1(z)$ and the control input $u(k)$ by $W_2(z)$. In general, $W_1(z)$ is chosen to be a lowpass function and $W_2(z)$ a small constant.

By the same token, the block diagram of the hybrid structure with acoustic feedback is illustrated in Figure 4. Dropping (z) for convenience, the input–output relation of the augmented plant corresponding to the hybrid structure is

$$
\begin{bmatrix} Z_1 \\ Z_2 \\ Z_3 \\ E_1 \\ E_2 \end{bmatrix} = \begin{bmatrix} W_1 & -W_1 P_1 & -W_1 P_2 \\ 0 & 0 & W_2 \\ 0 & W_3 P_1 & W_3 P_2 \\ 1 & -P_1 & -P_2 \\ 0 & 1 & P_3 \end{bmatrix} \begin{bmatrix} R \\ D \\ U \end{bmatrix}.
\tag{13}
$$

Hence, the suboptimal condition of the H_∞ hybrid controller can be shown to be

$$
\left\| \begin{bmatrix} W_1 HS & -W_1[P_1(1 - C_2 P_3) + C_2 P_2]HS \\ W_2 HR & W_2[C_2(z) - C_1(z)P_1]HS \\ W_3 HT & W_3[P_1(1 - C_2 P_3) + C_2 P_2]HS \end{bmatrix} \right\|_\infty < 1,
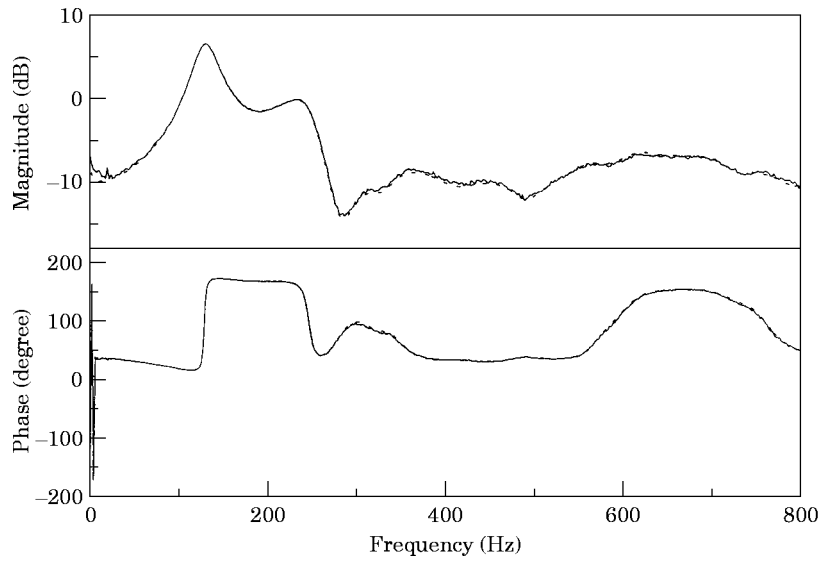\tag{14}
$$

Figure 5. The frequency response of the primary path plant. —, Measured curve; ---, modelled curve.

where

$$HS = (1 - C_2 P_3)/(1 - C_2 P_2 + C_1 P_2), \qquad HR = (C_2 - P_1 C_1)/(1 - C_2 P_3 + C_1 P_2),$$

and

$$HT = (P_1(1 - C_2 P_3) + C_2 P_2)/(1 - C_2 P_3 + C_1 P_2).$$

$HS(z)$ represents the transfer function from the disturbance to the downstream microphone output. $HT(z)$ is the transfer function associated with the *unstructured multiplicative uncertainty* [10] for the hybrid structure. In the structure, one weighs the error
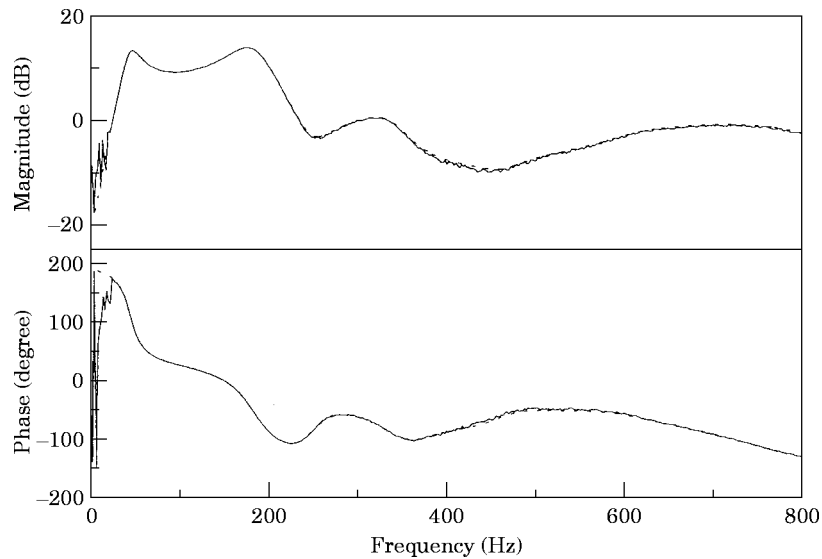

Figure 6. The frequency response of the secondary path plant. Key as for Figure 5.

TABLE 1

The models of the primary path, secondary path, and the acoustical feedback path of the duct identified by the ARX procedure

Primary path delay = 5, gain = −0·0641		Secondary path dealy = 1, gain = 0·9089		Acoustical feedback path delay = 1, gain = 0·0064	
zeros	poles	zeros	poles	zeros	poles
*− 1·7519	− 0·9446	− 0·5625 ± 0·6278i	− 0·8745	*− 1·7519	− 0·7250
*1·0369 ± 0·0706i	− 0·8639 ± 0·2333i	− 0·1412 ± 0·8068i	− 0·6287 ± 0·5669i	*− 1·0706	− 0·7521 ± 0·4749i
0·5948 ± 0·7568i	− 0·7408 ± 0·4752i	− 0·3310 ± 0·6297i	− 0·5297 ± 0·6706i	* 1·0389	− 0·8119 ± 0·2015i
0·6995 ± 0·3955i	− 0·5923 ± 0·6439i	0·2763 ± 0·8562i	− 0·3523 ± 0·7715i	0·9233	− 0·4763 ± 0·7045i
0·3147 ± 0·8005i	− 0·4231 ± 0·7432i	0·6592 ± 0·6741i	− 0·1286 ± 0·8607i	*2·0484 ± 1·8137i	− 0·3262 ± 0·7085i
0·1822 ± 0·7931i	− 0·2251 ± 0·8700i	*1·0633	0·3184 ± 0·8165i	*1·0837 ± 2·0421i	− 0·0983 ± 0·8864i
− 0·2188 ± 0·8650I	0·0814 ± 0·8060i	0·4148 ± 0·3587i	0·5475 ± 0·6839i	0·6327 ± 0·6693i	0·3223 ± 0·8489i
− 0·5331 ± 0·7142i	0·3095 ± 0·8262i	0·8927	0·7766 ± 0·4995i	0·5956 ± 0·6923i	0·2237 ± 0·7123i
− 0·7162 ± 0·4606i	0·5782 ± 0·7653i	− 0·4849	0·9629 ± 0·1435i	0·3143 ± 0·7870i	0·6590 ± 0·6588i
− 0·7992 ± 0·2037i	0·7640 ± 0·4875i	− 0·2726	0·6336 ± 0·3425i	− 0·8401 ± 0·3254i	0·7800 ± 0·4911i
− 0·7025	0·5964 ± 0·4081i	—	− 0·1661	− 0·0532 ± 0·7865i	0·8501 ± 0·2237i
—	0·9252 ± 0·1603i	—	—	− 0·4994 ± 0·4428i	0·9679 ± 0·1476i
—	0·9129	—	—	− 0·2340 ± 0·6325i	—
—	0·7411	—	—	—	—

* Denotes non-minimal phase zeros

signal $e_2(k)$ by a low-pass $W_1(z)$, the control input $u(k)$ by a small constant $W_2(z)$, and the downstream microphone output by a high-pass $W_3(z)$.

Recognizing that plant uncertainties and perturbations will affect the performance of ANC systems, it is desirable to quantitatively assess the performance robustness of the forging three ANC structures. This is done by defining the following performance robustness (PR) index of how performance of disturbance rejection varies with respect to plant perturbations:

$$PR = \lim_{\Delta P(z) \to 0} \frac{\Delta T_{yd}(z)/T_{yd}(z)}{\Delta P(z)/P(z)} = \frac{\partial \ln(T_{yd}(z))}{\partial \ln(P(z))} = \left(\frac{\partial T_{yd}(z)}{\Delta P(z)}\right)\left(\frac{P(z)}{T_{yd}(z)}\right), \qquad (15)$$

where the performance function T_{yd} denotes the transfer function from the disturbance $d(k)$ to the output $y(k)$ and $P(z)$ denotes the transfer function of the plant of interest. As can be seen in the definition, the larger the PR is, the worse the performance of disturbance rejection becomes in the presence of plant perturbations. In what follows, the PR indices PR_1, PR_2, and PR_3 stand for the PR indices associated with the primary path $P_1(z)$, the secondary path $P_2(z)$, and the acoustic feedback path $P_3(z)$, respectively, of the duct.

As will be seen shortly in the experimental results, a further improvement against plant perturbations can be achieved by the hybrid control structure. This interesting feature of hybrid control has also been noted by some other researchers [13, 14].

3. EXPERIMENTAL INVESTIGATIONS

Experiments were performed to compare the H_∞-based ANC structures in the presence of acoustic feedback problem. The H_∞ controller synthesis technique is employed to design an active electronic silencer for a duct. A rectangular duct of cross-section 0.25×0.25 m and length 1 m is used for the experiment, which renders the cutoff frequency 690 Hz. Within this control bandwidth, two fourth order Butterworth low-pass filters of cutoff frequency 600 Hz are employed as the antialiasing filter and reconstruction filter. The sampling rate is selected to be 2 kHz. The upstream reference microphone and error
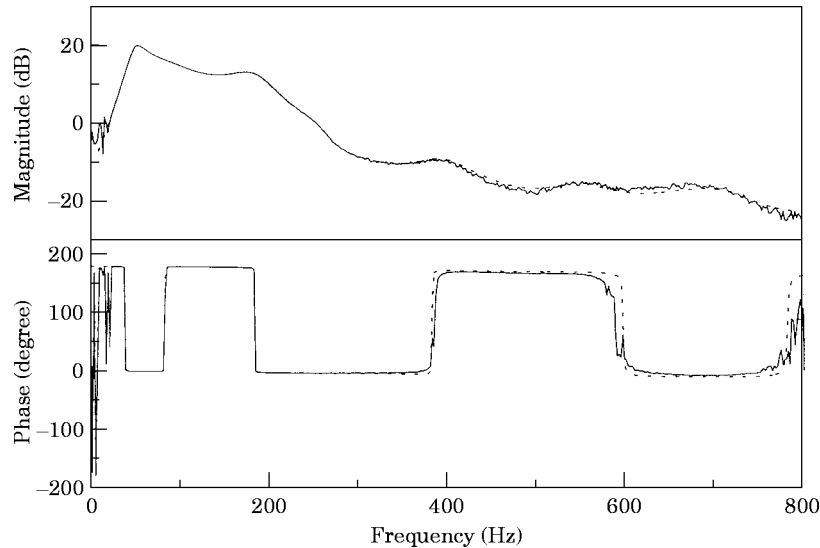

Figure 7. The frequency response of the acoustical feedback path plant. Key as for Figure 5.

TABLE 2

Experimental cases of the active electronic silencer for a duct

Case	Noise type	Algorithm	Control structure	*Order tap/step	Figure
**1	White noise	H_∞	Feedforward	–	8
2	White noise	H_∞	Feedback	–	9
3	White noise	H_∞	Feedforward	–	10
4	White noise	H_∞	Hybrid	–	12
		FULMS	Feedforward	30/0·0001	16(a)
5	White noise	Feedback neutralization		500/0·001	16(b)
6	Engine noise	H_∞	Hybrid	–	17

* Order, tap/step denotes either the order of the IIR filter for both the numerator and denominator, and the step size used in the FULMS algorithm, or the tap length of the FIR filter and the step size used in the feedback neutralization method.

** Case 1 is a reference case of purely feedforward control in the absence of acoustic feedback.

microphone are located at 0·25 m and 0·75 m, respectively, from the source end. It may first appear that the duct is very short compared to its cross-section, where the causality problem and excessive acoustic feedback may arise. This is indeed an unwilling compromise to make so that the the plant can be of sufficient low order below the cutoff frequency and numerical problems with the H_∞ calculation can be minimized. Besides, causality is a simplified criterion applicable to infinite-length ducts only. For the finite-length duct at hand, the complex dynamics of the acoustic system are reflected by the poles and zeros, but not simply the pure time delays as in the case of infinite-length ducts. On the other hand, the duct is lined with some fiberglass sound-absorbing material to provide appropriate damping for the system. The importance of passive damping that has often been overlooked in active design lies in not only high frequency attenuation but also the robustness of active control with respect to plant uncertainties [15]. With sufficient damping treatment, the order of plant uncertainty is generally less than that of the unlined duct. On the other hand, the error microphone is placed in the close vicinity of the control loudspeaker to form the so-called *collocated control*. In doing so, the waterbed effect in conjunction with non-minimal phase zeros and time delay can be alleviated [9, 16].
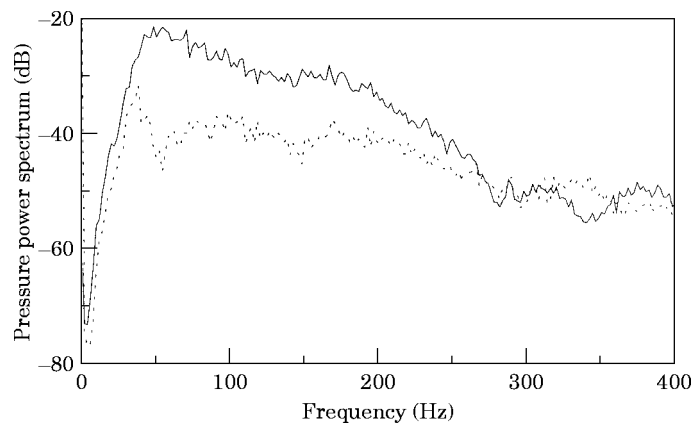

Figure 8. The residual sound pressure spectra of Case 1 for the white noise in the absence of acoustical feedback before and after ANC is activated by using the purely feedforward H_∞ controller. —, Control off; ---, control on.
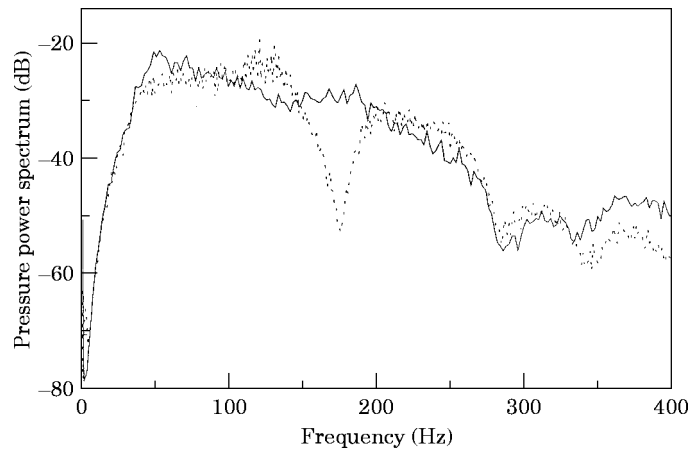
Figure 9. The residual sound pressure spectra of Case 2 for the white noise source when acoustical feedback is present before and after ANC is activated by using the H_∞ feedback controller. Key as for Figure 5.

In the experiment, the mathematical models of the primary path, the secondary path and acoustical feedback path are established via an ARX system identification procedure [17]. The identified poles and zeros of these three plants are listed in Table 1. The frequency responses of the primary path, the secondary path, and the acoustical feedback path are shown in Figures 5–7, respectively. On the basis of the plant models, the H_∞ synthesis procedure is applied to obtain the H_∞ controller. The controller is then coded into a digital filter on the platform of a floating-point DSP, TMS320C31. The experimental arrangements are illustrated in Figures 2(a), 3(a), and 4(a) for the feedback structure, the feedforward structure, and the hybrid structure, respectively. In addition, three synthetic as well as practical noise types, including a Gaussian white noise, an engine exhaust noise and an impact noise are chosen for comparing the different ANC structures. The experimental case design is shown in Table 2.

Case 1 is a reference case of purely feedforward H_∞ control, where the source voltage signal is used as the feedforward reference so that acoustic feedback can be neglected. It
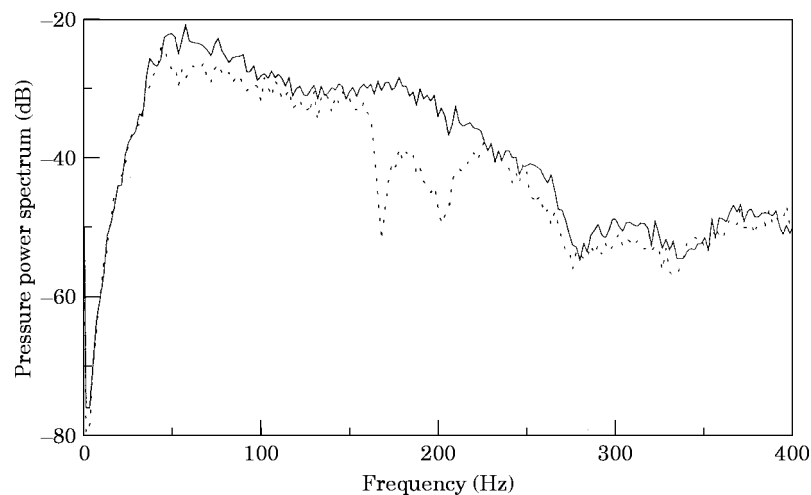

Figure 10. The residual sound pressure spectra of Case 3 for white noise source when acoustical feedback is present before and after ANC is activated by using the H_∞ feedforward controller. Key as for Figure 8.

TABLE 3

The poles and zeros of the feedback controller

delay = 0,   gain = −0·1280

zeros	*−2·9311	−0·8762	−0·9756	−0·7016 ± 0·2218i	−0·2417 ± 0·8509i
poles	−0·9801	−0·8531	−0·8023	−0·7190	−0·4830 ± 0·6829i
zeros	−0·4763 ± 0·7045i	−0·3582 ± 0·6160i	−0·7250	−0·3262 ± 0·7085i	−0·0983 ± 0·8864i
poles	−0·3866 ± 0·7704i	−0·3335 ± 0·6933i	−0·2206 ± 0·7853i	−0·1049 ± 0·8777i	−0·3871 ± 0·1128i
zeros	0·3223 ± 0·8489i	0·4660 ± 0·7756i	0·2237 ± 0·7123i	0·0044	0·0928
poles	0·3196 ± 0·8828i	−0·0003	0·3170 ± 0·7497i	0·2561 ± 0·5695i	0·4275 ± 0·7483i
zeros	0·6283 ± 0·7327i	0·5821 ± 0·5469i	0·6590 ± 0·6588i	0·4977 ± 0·2561i	0·6335
poles	0·2953 ± 0·3680i	0·6640 ± 0·6908i	0·6361 ± 0·6557i	0·4810	0·9754 ± 0·1493i
zeros	0·5192	0·8053 ± 0·4126i	0·7562 ± 0·5021i	0·9911	0·9272
poles	0·9818 ± 0·0441i	0·9924	0·9351	0·8664 ± 0·1298i	0·6888 ± 0·5185i
zeros	0·9603 ± 0·1314i	0·9579 ± 0·1476i	0·8501 ± 0·2237i	0·7822 ± 0·4891i	0·7800 ± 0·4911i
poles	0·8044 ± 0·4186i	0·8350 ± 0·4186i	0·7791 ± 0·5313i	0·7788 ± 0·4977i	–

* Denotes non-minimal phase zeros.

TABLE 4

The poles and zeros of feedforward controller

delay = 0,   gain = 0·3725

|					
zeros	*−1·0125	−0·9756	−0·7367 ± 0·3400i	−0·5724 ± 0·5447i	−0·2417 ± 0·8059i
poles	−0·2228 ± 0·7830i	−0·7419 ± 0·2637i	−0·5260 ± 0·4643i	−0·5420 ± 0·3497i	−0·5067
zeros	−0·3582 ± 0·6160i	0·1132 ± 0·8661i	0·4660 ± 0·7756i	0·5821 ± 0·5469i	0·8998 ± 0·4702i
poles	0·2704 ± 0·9413i	0·1332 ± 0·8898i	0·3838 ± 0·7692i	−0·1020	0·6763 ± 0·6445i
zeros	0·7822 ± 0·4891i	0·9603 ± 0·1314i	0·9462	0·6335	−0·1020
poles	0·8539 ± 0·5105i	0·9743 ± 0·1807i	0·4790	0·9604	0·9621

* Denotes non-minimal phase zeros
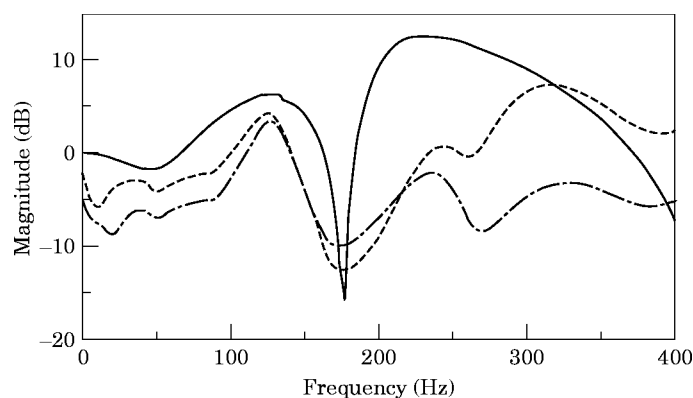
Figure 11. The predicted performance function $T_{yd}(z)$ of three active noise controllers for the duct. —, Feedforward controller; - - - -, feedforward controller in the presence of acoustical feedback; $- \cdot - \cdot$, hybrid controller in the presence of acoustical feedback.

can be seen from the result of Figure 8 that significant attenuation (approximately 5–20 dB) is obtained in the frequency range 40–200 Hz. In Cases 2–4, the signal detected by an upstream microphone is used as the feedforward reference so that the effect of acoustic feedback can no longer be ignored in the feedforward and the hybrid structures. In these cases, the H_∞ ANC systems are employed for attenuating the white noise. In the experimental results shown in Figure 9, it can be observed that the noise attenuation reaches approximately 20 dB at 175 Hz, but the effective band appears quite narrow (145–180 Hz). The poles and zeros of the feedback controller are listed in Table 3. The total attenuation within the dominant band 0–400 Hz is found to be 2·02 dB. The experimental results of the H_∞ feedback control show similar waterbed effect to that of the H_2 control [18] and the pole placement method [19], and in these cases only narrowband attenuation can be achieved. It is found in the H_2 method that noise attenuation is obtained in the band 200–320 Hz at the expense of creating peaks at higher frequencies. In the pole placement technique, the attenuation is observed at the first two modes (47 Hz and 95 Hz, respectively).
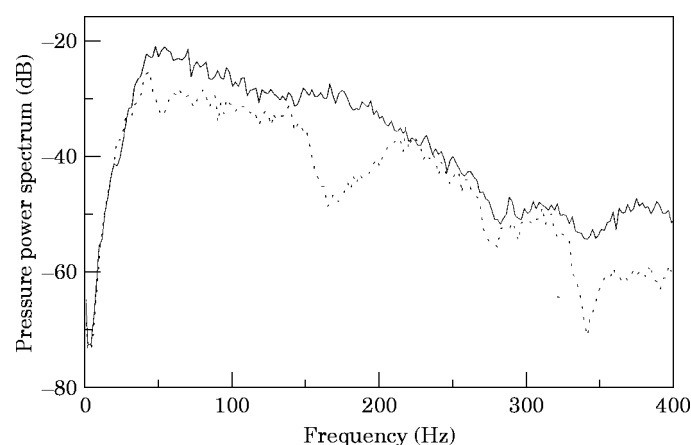

Figure 12. The residual sound pressure spectra of Case 4 for the white noise source when acoustical feedback is present before and after ANC is activated by using the H_∞ hybrid controller. Key as for Figure 8.

TABLE 5

The poles and zeros of hybrid controller

Feedforward part delay = 0, gain = 0·1108		Feedback part delay = 0, gain = −0·1237	
zeros	poles	zeros	poles
−0·9801	−0·9803	*−3·3641	−0·9803
−0·8536	−0·8398	−0·8879	−0·8398
−0·9756	−0·8264	−0·9756	−0·8264
−0·7250	−0·7364	−0·7666	0·7364
−0·5956 ± 0·6923i	−0·5934 ± 0·6922i	−0·5836 ± 0·7081i	−0·5934 ± 0·6922i
−0·4763 ± 0·7045i	−0·4817 ± 0·6807i	−0·7250	−0·4817 ± 0·6807i
−0·4439 ± 0·7825i	−0·4482 ± 0·7854i	−0·4413 ± 0·7938i	−0·4482 ± 0·7854i
−0·0983 ± 0·8864i	−0·3850 ± 0·7648i	−0·3084 ± 0·8506i	−0·3850 ± 0·7648i
−0·3262 ± 0·7085i	−0·2998 ± 0·8688i	−0·4763 ± 0·7045i	−0·2998 ± 0·8688i
−0·3999 ± 0·7295i	−0·3316 ± 0·6935i	−0·1571 ± 0·9104i	−0·3316 ± 0·6935i
−0·2992 ± 0·8666i	−0·1520 ± 0·9215i	−0·3582 ± 0·6160i	−0·1520 ± 0·9215i
−0·3582 ± 0·6160i	−0·2214 ± 0·7848i	−0·2417 ± 0·8059i	−0·2214 ± 0·7848i
−0·1497 ± 0·9207i	−0·1010 ± 0·8757i	−0·3262 ± 0·7085i	−0·1010 ± 0·8757i
−0·2417 ± 0·8059i	0·0681 ± 0·9241i	0·0637 ± 0·9400i	0·0681 ± 0·9241i
−0·1020	0·1336 ± 0·8844i	−0·0983 ± 0·8864i	−0·1336 ± 0·8844i
0·0704 ± 0·9221i	−0·1694	0·1132 ± 0·8661i	−0·1694
0·1132 ± 0·8661i	0·2515 ± 0·8673i	0·2739 ± 0·8749i	0·2515 ± 0·8673i
0·3223 ± 0·8489i	0·3180 ± 0·8784i	−0·0670	0·3180 ± 0·8784i
0·2237 ± 0·7123i	0·0001	0·3223 ± 0·8489i	0·0001
0·2653 ± 0·8560i	0·0331	0·5090 ± 0·8052i	0·0331
0·5036 ± 0·7872i	0·3062 ± 0·7624i	0·4660 ± 0·7756i	0·3062 ± 0·7624i
0·4660 ± 0·7756i	0·2316 ± 0·5719i	0·2237 ± 0·7123i	0·2316 ± 0·5719i
0·4152 ± 0·6802i	0·5048 ± 0·7883i	0·2995 ± 0·5814i	0·5048 ± 0·7883i
0·6590 ± 0·6588i	0·4288 ± 0·7452i	0·6203 ± 0·7336i	0·4288 ± 0·7452i
0·9579 ± 0·1476i	0·3359 ± 0·5933i	0·5821 ± 0·5469i	0·3359 ± 0·5933i
0·8501 ± 0·2237i	0·6636 ± 0·6933i	0·6590 ± 0·6588i	0·6636 ± 0·6933i
*1·0295	0·6362 ± 0·6564i	0·8454 ± 0·5052i	0·6362 ± 0·6564i
0·9975	0·9702 ± 0·1803i	*1·1395	0·9702 ± 0·1803i

* Denotes non-minimal phase zeros.

In contrast to the feedback structure, a broader band of attenuation can be obtained by using the feedforward structure. In Figure 10, significant attenuation up to approximately 12–22 dB of the random noise has been achieved throughout the band 150–220 Hz by using the feedforward control and total attenuation within the band 0–400 Hz is found to be 2·96 dB. The poles and zeros of feedforward controller are listed in Table 4.

In viewing the above results of noise attenuation, it is instructive to plot the transfer functions between the disturbance and the downstream microphone of the three ANC structures (Figure 11). The feedback structure displays only very narrowband noise rejection, as have been confirmed by the experimental results. The feedforward structure and the hybrid structure appear to have comparable performance, both better than that of the feedback control. Nevertheless, it is noteworthy that the experimental results reported in Figure 12 show considerable improvement of the hybrid structure over the feedforward structure. Attenuation has been achieved in two regions, 40–200 Hz and 330–400 Hz, by using the hybrid control and the poles and zeros of hybrid controller are listed in Table 5. Attenuation up to approximately 20 dB is obtained in the first region and 18 dB in the second region. The total attenuation within the band 0–400 Hz is found
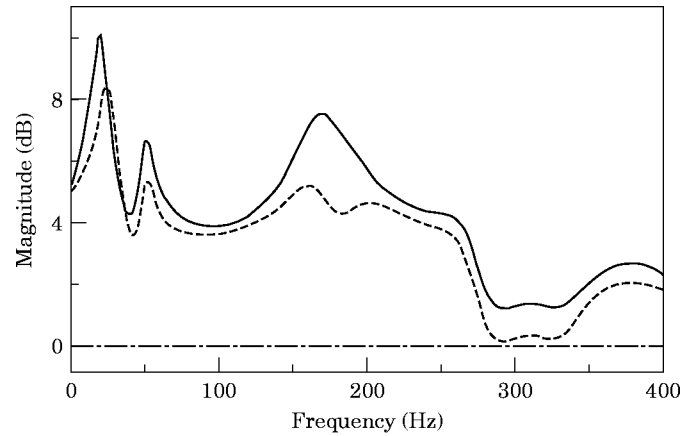
Figure 13. The performance robustness index PR_1 of three active noise controllers for the duct in the presence of acoustical feedback. —, Feedback controller; - - - -, feedforward controller; $- \cdot - \cdot$, hybrid controller.

to be 3·42 dB. This result is of comparable order with the theoretical prediction except some minor discrepancy due to modeling error by using the ARX procedure. Some additional insights can be obtained by calculating the PR indices, as shown in Figures 13–15. The indices PR_1, PR_2 and PR_3 of the feedforward structure are the largest among the ANC structures in most of the frequencies, while the indices PR_1 and PR_2 of the feedback structure are the smallest. That is, the performance of the feedforward control is the most susceptible to plant uncertainties among the ANC structures, while the performance of the feedback control is the most robust against the plant perturbations. As a compromise between the feedforward control and the feedback control, the robustness of performance of the hybrid control is partially improved by the introduction of the feedback structure. Hence, the experimental results of the hybrid control agree more closely with the predicted performance than the feedforward control.
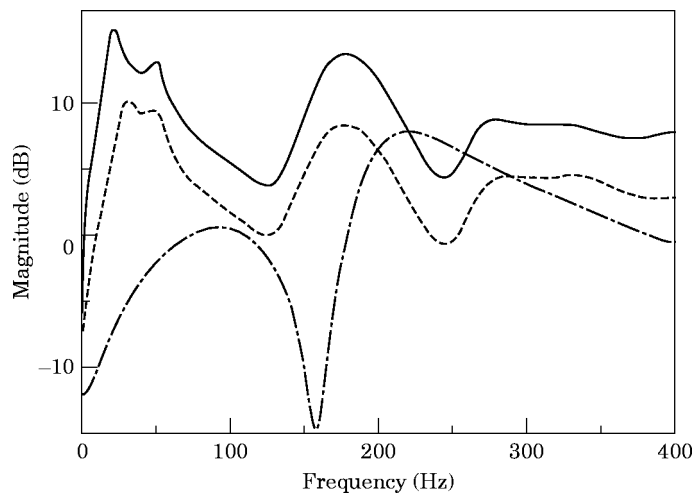

Figure 14. The performance robustness index PR_2 of the three active noise controllers for the duct in the presence of acoustical feedback. Key as for Figure 13.
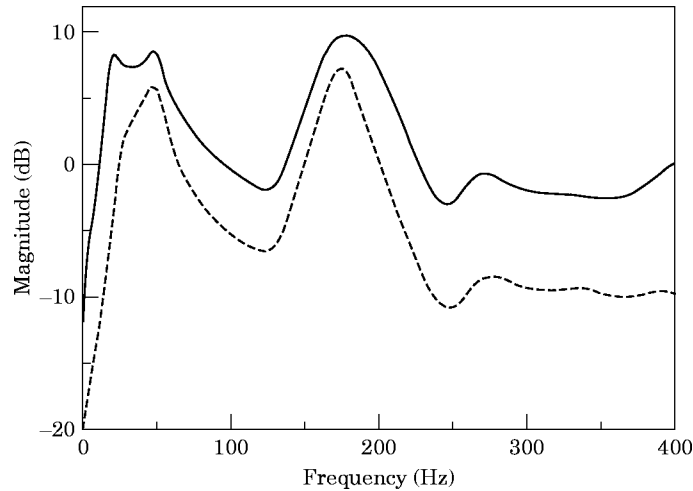
Figure 15. The performance robustness index PR_3 of active noise feedforward and hybrid controller for the duct in the presence of acoustical feedback. - - - -, Feedforward controller; ——, hybrid controller.

In the fifth case, two commonly used methods for dealing with acoustical feedback, the FULMS method and the feedback neutralization method, are employed in the present experiment for comparison with the proposed techniques. The details of these two methods can be found in reference [12] and are omitted here for brevity. Both the orders of the numerator and the denominator of the IIR filter used in FULMS method are 30. The tap length of FIR controller in the feedback neutralization technique is 300. The step size is 0·0001 in the two methods. The FULMS method produces 3–20 dB attenuation in the frequency range 50–200 Hz (Figure 16(a)). Total attenuation within the band 0–400 Hz is found to be 2·42 dB. The result was obtained 1 min after the active control was activated. However, a strong peak was found at 235 Hz in the spectrum of the FULMS algorithm. It appears that the FULMS method is prone to stability problems for the algorithm is trapped in a local minimum (because its performance index is generally not quadratic) and
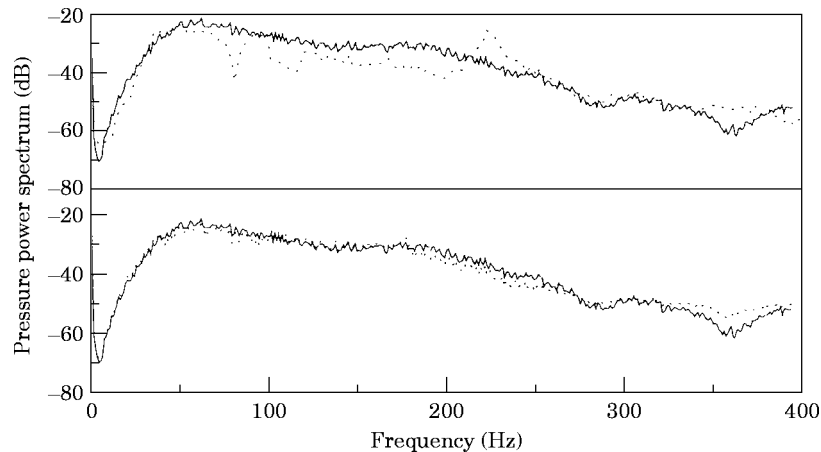
Figure 16. The residual sound pressure spectra of Case 5 for the white noise source when acoustical feedback is present before and after ANC is activated: (a) FULMS method; (b) the feedback neutralization method. Key as for Figure 8.
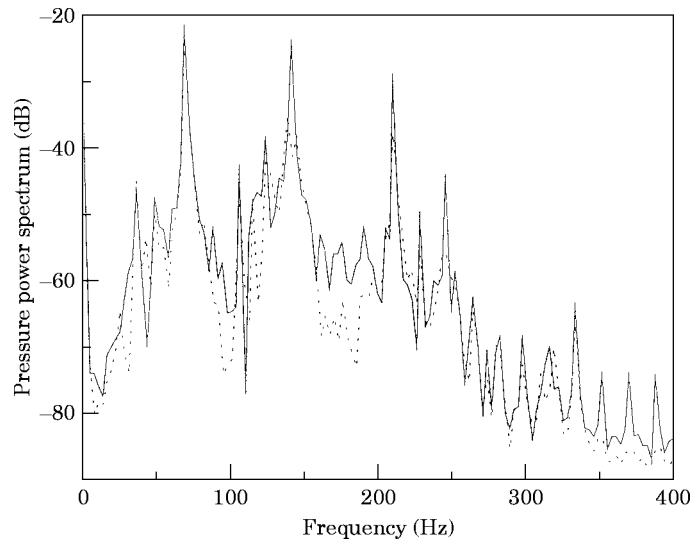
Figure 17. The residual sound pressure spectra of Case 8 for the engine exhaust noise when acoustical feedback is present before and after ANC is activated by using the H_∞ hybrid controller. Key as for Figure 8.

the control drifts away slowly so that the system can be unstable. As pointed out by the reviewer, the problem with stability may be solved by using the leaky LMS algorithm [12]. On the other hand, the experimental results of the feedback neutralization method are shown in Figure 16(b). Almost no attenuation can be obtained by using this method, the detrimental effect of acoustic feedback being evident from these results. Irrespective of which method used, the performance of noise attenuation is significantly degraded in comparison with the purely feedforward control in Case 1.

In the last case dealing with more practical noise, an exhaust noise from a 2000 cm³ gasoline engine running at 4000 r.p.m., is investigated by using the H_∞ hybrid controller. The results are shown in Figure 17. Significant attenuation, approximately 20 dB and 12 dB can be observed at the second and third peak of the power spectra and total attenuation within the band 0–400 Hz is found to be 5·43 dB.

4. CONCLUSIONS

Three ANC structures of active noise cancellation for ducts: feedback control, feedforward control, and hybrid control have been compared in this paper by using a general framework of the H_∞ robust control theory. The H_∞ synthesis procedure incorporates, without special treatment, the acoustic feedback path that is usually a plaguing problem to feedforward control design. Three ANC systems have been practically implemented by using a DSP.

The characteristics of each ANC structure, as indicated in the experimental results, can be summarized as follows. The main advantage of the feedback control is that no reference input is needed so that the acoustic feedback problem can be avoided. Nevertheless, the feedback control suffers from the waterbed effect due to time delay and non-minimum phase zeros and only narrowband noise rejection is achievable. For a high order plant such as a duct in our case, feedforward control appears to be a more viable approach for broadband noise rejection at the expense of performance robustness against plant uncertainties. Alternatively, hybrid control can be used to simultaneously achieve broadband noise rejection and robust performance. In comparison with the

feedforward control, the feedback control, and the well-known FULMS method, the experimental results of the H_∞ hybrid controller exhibit excellent performance for suppressing stationary and transient noises, even in the presence of serious acoustic feedback. Nevertheless, it is remarked that the experimental duct is very short compared to its cross-section in the study, which might violate the causality constraint that is generally used as a design criterion of an infinite-length duct. The experimental results may be improved with a longer duct, provided the increased order of plant models is not an issue.

Despite the preliminary success, the H_∞ hybrid controller is a fixed controller that may not be able to accommodate excessive plant perturbations, e.g., large temperature variations in a muffler. It is reported in Eriksson's work [20] that an adaptive controller with online plant modelling is capable of tracking such plant variations (despite some drawbacks detailed in the book by Kuo and Morgan [12]). From the same perspective, combination of the fixed and the adaptive controllers may make it possible to improve the robustness and thus will be explored in a future study.

REFERENCES

1. S. J. ELLIOT and P. A. NELSON 1993 *IEEE Signal Processing Magazine* **10**, 12–35. Active noise control.
2. C. R. FULLER and A. H. VON FLOTOW 1995 *IEEE Control Systems Magazine* **2**, 9–19. Active control of sound and vibration.
3. J. C. BURGESS 1981 *Journal of the Acoustical Society of America* **70**, 715–726. Active adaptive sound control in a duct: a computer simulation.
4. L. J. ERIKSSON 1990 *Journal of the Acoustical Society of America* **89**, 257–265. Development of the filter-u algorithm for active noise control.
5. V. EGHTESADI and H. G. LEVENTHALL 1982 *Journal of the Acoustical Society of America* **71**, 608–611. Active attenuation of noise: the monopole system.
6. J. C. DOYLE, K. GLOVER, P. KHARGONEKAR, and B. A. FRANCIS 1989 *IEEE Transactions on Automatic Control* **34**, 832–847. State space solution to standard H_2 and H_∞ control problems.
7. P. A. IGLESIAS and K. GLOVER 1991 *International Journal of Control* **54**, 1031–1073. State-space approach to discrete-time H_∞ control.
8. I. YAESH and U. SHAKED 1991 *IEEE Transactions on Automatic Control* **36**, 1264–1271. Transfer function approach to the problems on discrete-time systems: H_∞ optimal linear control and filtering.
9. J. C. DOYLE, B. A. FRANCIS and A. R. TANNENBAUM 1992 *Feedback Control Theory*. New York: Macmillan Publishing Company.
10. F. B. YEH and C. D. YANG 1992 *Post Modern Control Theory And Design*. New York: Eurasia.
11. M. C. TSAI and C. S. TSAI 1995 *International Journal of Control* **5**, 155–173. A transfer matrix framework approach to the synthesis of H_∞ controllers.
12. S. M. KUO and D. R. MORGAN 1996 *Active Noise Control Systems Algorithms and DSP Implementations*. New York: John Wiley.
13. M. MORARI and E. ZAFIRIOU 1989 *Robust Process Control*. Englewood Cliffs, N.J.: Prentice-Hall.
14. H. IMAI and H. HAMADA 1995 *Proceedings of International Symposium on Active Control of Sound and Vibration*, '95 875–880. Active noise control system based on the hybrid design of feedback and feedforward control.
15. R. GUELER, A. H. FLOTOW and D. W. VOS 1993 *Journal of Guidance*, *Control and Dynamics* **16**, 662–667. Passive damping for robust feedback control of flexible structures.

16. G. F. FRANKLIN, J. D. POWELL and A. EMAMI-NAEINI 1994 *Feedback Control of Dynamic Systems*. Reading, M.A.: Addison-Wesley.

17. L. LJUNG 1987 *System Identification*: *Theory for the User*. Englewood Cliffs, N.J.: Prentice-Hall.

18. J. HONG, J. C. AKERS, R. VENUGOPAL, M. N. LEE, A. G. SPARKS, P. D. WASHABAUGH and D. S. BERNSTEIN 1996 *IEEE Transactions on Control Systems Technology* **4**, 283–291. Modeling, identification and feedback control noise in an acoustic duct.

19. A. J. HULL, C. R. RADCLIFFE and S. C. SOUTHWARD 1993 *ASME Journal of Dynamic Systems, Measurement and Control* **115**, 488–494. Global active noise control of a one-dimensional acoustic duct using a feedback controller.

20. L. J. ERIKSSON and M. C. ALLIE 1989 *Journal of the Acoustical Society of America* **85**, 797–802. Use of random noise for on-line transducer modeling in an adaptive active attenuation system.